

Activation energy of reaction velocity constant was found to be 1.3 ~ 1.6 eV.

4. Mo-gate MOSFET's, having good stability in short term BT stressing, were fabricated with satisfactory reproducibility.

Acknowledgment

The authors would like to express their thanks to Drs. D. Shinoda and H. Muta for their encouragement, to Dr. K. Higuchi for helpful discussions, and to Mr. I. Nagashima and Mr. C. Takekawa for device fabrication.

Manuscript submitted Feb. 22, 1980; revised manuscript received July 28, 1980.

Any discussion of this paper will appear in a Discussion Section to be published in the December 1981 JOURNAL. All discussions for the December 1981 Discussion Section should be submitted by Aug. 1, 1981.

Publication costs of this article were assisted by Nippon Electric Company, Limited.

REFERENCES

1. M. Kondo, T. Mano, F. Yanagawa, K. Kikuchi, T. Amazawa, K. Kiuchi, N. Ieda, and H. Yoshimura, *IEEE J. Solid-State Circuits*, **sc-13**, 611 (1978).

2. T. Ohgishi, A. Doi, T. Akiyama, and N. Enomoto, *ibid.*, **sc-13**, 355 (1978).
3. H. Ishikawa, M. Yamamoto, T. Nakamura, N. Toyokura, F. Yanagawa, K. Kiuchi, and M. Kondo, *IEDM Tech. Digest*, p. 358 (1979).
4. F. Yanagawa, K. Kiuchi, T. Hosoya, T. Tsuchiya, T. Amazawa, and T. Mano, *ibid.*, p. 362 (1979).
5. F. Yanagawa, T. Amazawa, and H. Oikawa, Proc. 10th Conf. Solid-State Devices, Tokyo, 1978; *Jpn. J. Appl. Phys. Suppl.*, **18**, 237 (1979).
6. D. R. Kerr, J. S. Logan, P. J. Burkhardt, and W. A. Pliskin, *IBM J. Res. Dev.*, **8**, 376 (1964).
7. A. Rohatgi, S. R. Butler, and F. J. Feigl, *This Journal*, **126**, 149 (1979).
8. J. Monkowski, J. Stach, and R. E. Tressler, *ibid.*, **126**, 1129 (1979).
9. M. Koyanagi, T. Hayashida, N. Yamamoto, and N. Hashimoto, Abstract 153, p. 409, The Electrochemical Society Extended Abstracts, Boston, Mass., May 6-11, 1979.
10. E. Yon, W. H. Ko, and A. B. Kuper, *IEEE Trans. Electron Devices*, **ed-13**, 276 (1966).
11. R. N. Ghoshtagore, *Solid-State Electron.*, **18**, 399 (1975).
12. A. E. Owen and R. W. Douglas, *J. Soc. Glass Technol.*, **43**, 159 (1959).
13. Y. Komiya, Y. Tarui, and K. Nagai, *Bull. Electro-techn. Lab.*, **30**, 34 (1966) (in Japanese).
14. E. H. Snow, A. S. Grove, B. E. Deal, and C. T. Sah, *J. Appl. Phys.*, **36**, 1664 (1965).

Silicon by Sodium Reduction of Silicon Tetrafluoride

A. Sanjurjo,* L. Nanis,* K. Sancier, R. Bartlett, and V. Kapur*

SRI International, Menlo Park, California 94025

ABSTRACT

High purity silicon can be prepared from the reaction of Na with SiF₄ to form Si and NaF. The SiF₄ is obtained from inexpensive H₂SiF₆ by precipitation and decomposition of Na₂SiF₆. Concentrations of B and P are each in the 0.1 ppm wt range in the product Si, separated from NaF by aqueous leaching.

Silicon is an important material in modern semiconductor technology and is finding increased use in solar cells for the photovoltaic generation of electricity. Each application presents special requirements for the purity of the silicon. Certain elements (Ti, Zr, Mo, V, Cr, Fe) have been found to be detrimental to the operation of silicon solar cells by acting as recombination traps when present in concentrations of as little as 0.01-1 ppba (1, 2). Low cost silicon of high purity is needed to foster the continued development of solar photovoltaic systems. With today's technology, approximately 20% of the total cost for the manufacture of a solar cell is ascribed to the silicon material produced by the conventional hydrogen reduction of chlorosilanes. It has been estimated (3) that the cost of silicon must be reduced from its present level of at least \$70/kg to about \$14/kg (in 1980 dollars) to achieve acceptance for use in solar photovoltaic panels. We have developed a process that offers a pathway to an industrial method that satisfies this cost requirement. The starting material is fluosilicic acid, H₂SiF₆, a low cost waste by-product of the phosphate fertilizer industry (4). SiF₄ gas is prepared from H₂SiF₆ and is reacted with sodium metal to produce a mixed reaction product consisting of Si and NaF. Aqueous leaching is used to separate NaF from granular Si.

The SiF₄-Na Process

The overall process consists of three major steps: step 1, precipitation of Na₂SiF₆, followed by SiF₄ gen-

eration; step 2, Na reduction of SiF₄; and step 3, separation of Si from the Si-NaF mixture. A flow diagram of the process steps is shown in Fig. 1. The sequence of reactions is described below.

Generation of SiF₄ (step 1).—Fluosilicic acid (H₂SiF₆) of commercial grade [23 weight percent (w/o)] was used directly as received without purification or special treatment. Sodium fluosilicate, Na₂SiF₆, was precipitated by adding solid sodium fluoride directly to the as-received H₂SiF₆. The mixture was stirred overnight at room temperature in a polypropylene tank. The supernatant liquid, containing mostly HF and some H₂SiF₆, was decanted, and the Na₂SiF₆ precipitate was filtered on a plastic Buchner funnel. The fluosilicate was washed with cold distilled water to remove HF and H₂SiF₆ and dried in an oven at 200°C. A minimum yield of 92% was obtained for 1 kg batches of pure Na₂SiF₆ as determined by x-ray diffraction. The product Na₂SiF₆ is a nonhygroscopic white powder that is very stable at room temperature and thus provides an excellent means for storing the silicon source before it is decomposed to SiF₄.

As SiF₄ is needed, the Na₂SiF₆ can be thermally decomposed (Fig. 1) at 650°C in a graphite-lined, gas-tight stainless steel retort. In separate experiments, it was determined that SiF₄ gas at a pressure of 0.4 atm is in equilibrium at 650°C with solid Na₂SiF₆ and NaF. Accordingly, gaseous SiF₄ evolved at 650°C was condensed as a white solid in a storage cylinder cooled by liquid nitrogen, attached to the retort. The SiF₄ gas was allowed to expand by warming of the storage cylinder

* Electrochemical Society Active Member.

Key words: silicon, solar cells, sodium, silicon tetrafluoride.

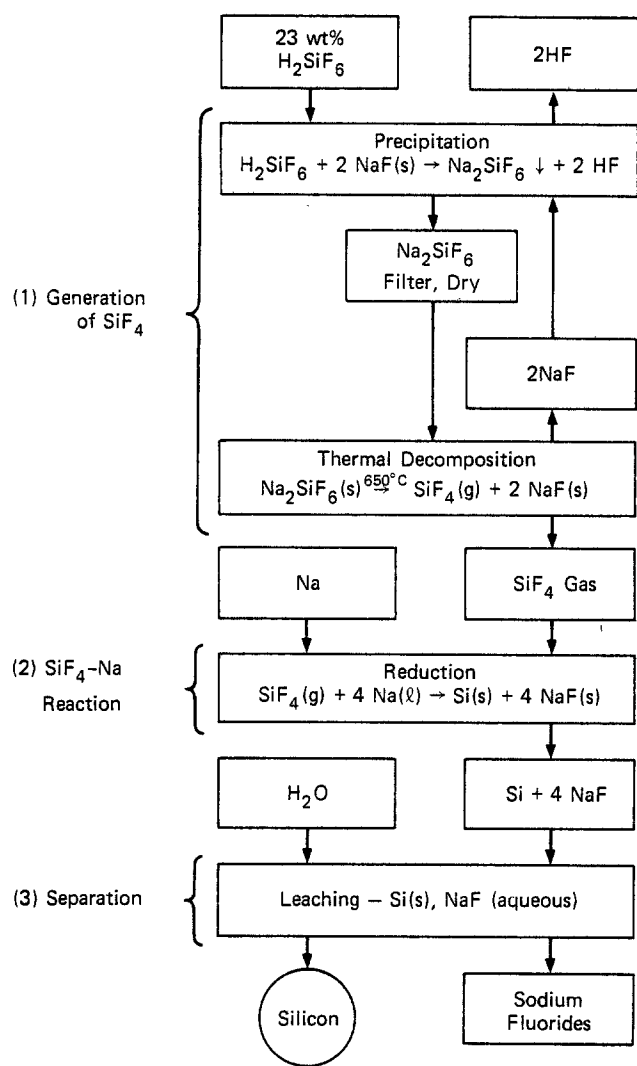


Fig. 1. Three-step method for silicon production

to room temperature and was fed into the reactor as needed. SiF_4 gas prepared in this manner was determined by mass spectrometric analysis to be more pure than commercial grade SiF_4 , as shown in Table I. Ions formed from the sample gas were identified from the observed mass numbers, isotopic distribution, and threshold appearance potentials. The detection limit was better than 0.005%. Positively identified gaseous impurities are listed in Table I; no metallic impurities were detected. Peaks corresponding to B compounds, such as BF_3 , were specially checked, but none were found.

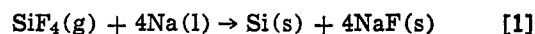
Although the SiF_4 produced from H_2SiF_6 had less impurity, the commercial grade SiF_4 was also used for experimental convenience. The possible presence of metallic impurities in commercial SiF_4 was determined by bubbling the gas through high purity H_2O and heating the resulting slurry with an excess of HF to drive off Si as SiF_4 . The final clear solution was then analyzed by plasma emission spectroscopy (PES). The

Table I. Mass spectrometric analysis of SiF_4

Ion	SiF_4 prepared at SRI from H_2SiF_6 (%)	SiF_4 commercial (%)
SiF_3^+	96.9	93.6
Si_2OF_6^+	3.04	4.24
SiOF_2^+	—	1.79
CCl_3^+	—	0.159
SO_2F_2^+	0.076	0.098
$\text{Si}_2\text{O}_2\text{F}_4^+$	—	0.081
SO_2^+	—	0.035

results are listed in Table II, together with PES analysis of the waste by-product H_2SiF_6 and the NaF used to precipitate Na_2SiF_6 (step 1, Fig. 1). Comparison of the first two columns of Table II with column three shows that the concentrations of some elements, e.g., Li, B, V, Mn, Co, K, and Cu, were unchanged by precipitation of Na_2SiF_6 , whereas the elements Mg, Ca, Al, P, As, and Mo were diminished by a factor of 5-10. Some elements were concentrated into the Na_2SiF_6 , namely Cr, Fe, and Ni. The fourth column in Table II is representative of the impurity content to be found in SiF_4 gas prepared on a commercial scale. The low content of P is of special significance for both semiconductor and solar cell applications. Elements known to reduce solar cell efficiency (V, Cr, Fe, Mo) are uniformly low in commercial grade SiF_4 . Only Mn, As, and Al are of comparable concentrations in both Na_2SiF_6 and SiF_4 at the 1 ppm or less level.

SiF₄-Na reaction (step 2).—The central operation of the pure Si process (step 2, Fig. 1) is the reduction of SiF_4 by Na according to the reaction



Although this reaction is thermodynamically favored at room temperature ($\Delta G^\circ_{298\text{K}} = -146$ kcal/mole Si), it has been found experimentally that Na has to be heated to about 150°C before any appreciable reaction can be observed. Once the reacting has been initiated, the released heat ($\Delta H^\circ_{298\text{K}} = -164$ kcal/mole Si) raises the temperature of the reaction Na, which in turn increases the reaction rate. Under adiabatic conditions, a temperature of 2200 K is predicted for reaction [1] with the stoichiometric quantities of SiF_4 and Na. In practical reactors, rapid consumption of gaseous SiF_4 produces a pressure decrease. The kinetic behavior of reaction [1] is complex because of the interplay of several factors, e.g., pressure of SiF_4 , vaporization of Na, local temperature, porosity of two solid products, and transport of SiF_4 and Na vapor through the product crust that forms on the liquid Na.

Although only preliminary studies have been made of the kinetics, the general features of reaction [1] have been surveyed. In a series of experiments to estimate reaction temperatures, 5g of Na were loaded in a Ni crucible (3 cm ID, 4 cm high) and heated in SiF_4 initially at 1 atm pressure. The Na surface tarnished at around 130°C , with the formation of a thin brown film. As the temperature increased, the color of the surface film gradually changed from light brown to brown and finally to almost black. The SiF_4 -Na reaction became rapid at $160^\circ \pm 10^\circ\text{C}$ and liberated a large amount of heat, as indicated by a sudden rise in re-

Table II. Plasma emission spectroscopy analysis, parts per million (wt)

Element	H_2SiF_6^a	NaF^b	Na_2SiF_6	SiF_4^c
Li	0.1	—	0.2	0.01
Na	460	—	—	1.8
K	9.0	—	8.0	0.3
Mg	55	—	6.4	2.3
Ca	110	10	18	1.6
B	1.0	—	0.8	<0.01
Al	8.0	<2.5	1.3	1.2
P	33	—	5	0.08
As	8.8	—	0.2	0.28
V	0.3	<5	0.3	<0.01
Cr	0.8	<3.5	8.8	<0.01
Mn	0.2	<4	0.4	0.16
Fe	13	>7	38	0.04
Co	0.54	—	0.7	<0.01
Ni	1.17	<8	4.2	<0.01
Cu	0.12	<4	0.6	<0.01
Zn	1.4	—	1	<0.01
Pb	14.5	—	5	0.03
Mo	11	—	1.0	<0.01

^a 23 w/o waste by-product of phosphate fertilizer production.

^b Emission spectroscopy.

^c Commercial grade.

^d Major line.

action temperature. As shown in Fig. 2, the pressure in the reactor typically decreased slightly until the temperature increased sharply, with an associated rapid decrease in SiF_4 pressure. The reaction lasts for several seconds only. For SiF_4 pressures below 0.3 atm, the reaction mass was observed to glow at a dull red heat. For higher pressure, a characteristic flame was observed. The shortest reaction time (20 sec) and the highest temperatures (about 1400°C) were obtained when the initial pressure of SiF_4 was around 1 atm. In addition, complete consumption of Na was obtained for 1 atm SiF_4 . When scale-up of this reaction was attempted by loading larger amounts of Na, it was found that as the depth of the Na pool increased, the amount of Na remaining unreacted also increased. The product formed a crust on top of the Na surface, building a diffusion barrier for the reactants. As the barrier thickness increased, the reaction slowed and eventually stopped.

On the basis of preliminary studies of the parameters that affect reaction [1], a system was developed that is capable of producing Si at the rate of 0.5 kg/hr in a batch mode. The reactor is shown schematically in Fig. 3. The upper section of the Na dispenser is coated internally with epoxy resin on all Pyrex glass surfaces that may contact Na.

Sodium chips were prepared by feeding 225g blocks of sodium (6 cm diam rod, cut longitudinally) into a food processor using a blanket of argon to minimize contact with atmospheric oxygen and moisture. While Na chips were being introduced into the top of the storage chamber of the dispenser (2 kg capacity), dry argon flowed up through the chamber. The Na chips were transferred from the storage chamber to the reactor by means of a horizontal "hoe" mechanism. Downward flow of Na chips in the storage chamber was aided by agitation of the vertical rod.

The lower section of the reactor was made of Inconel (20 cm diam, 90 cm high) and was fitted with a sheet nickel liner (18 cm diam, 60 cm high) and an inner liner of sheet Grafoil (18 cm diam, 90 cm high). The outside of the Inconel reactor was wrapped with four sets of heavy duty electrical heating tapes (rated for use to 800°C), which were covered with Kaowool insulation (1.3 cm thick). The top of the Inconel reactor and the flanges that connect to the Pyrex Na dispensing section were water cooled.

In operating the reactor, the system was first evacuated, then filled with SiF_4 gas to a pressure of about 1

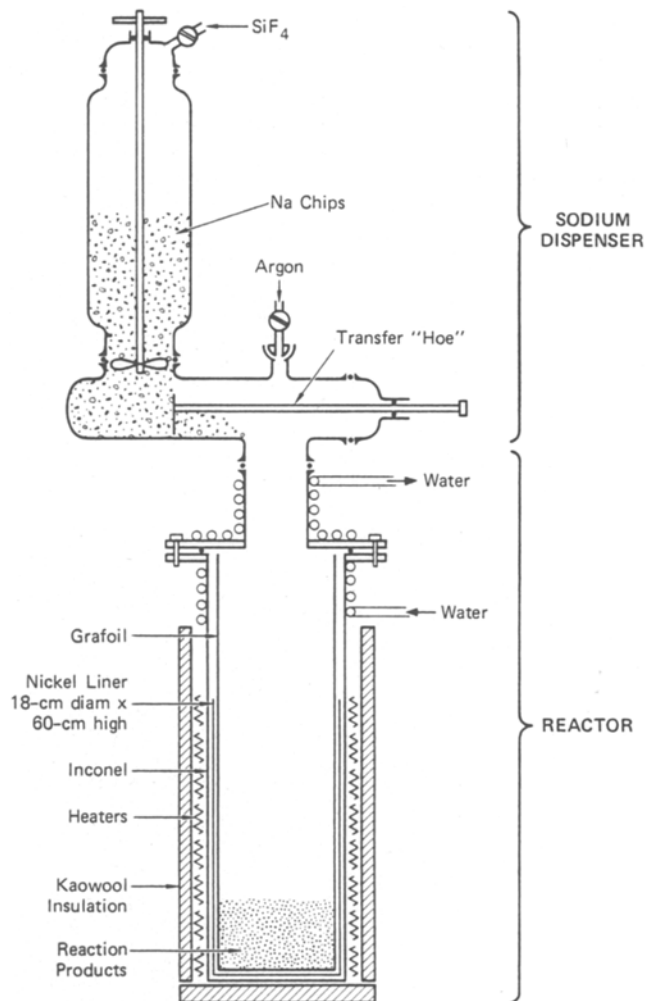


Fig. 3. Schematic of 18 cm diam Inconel reactor

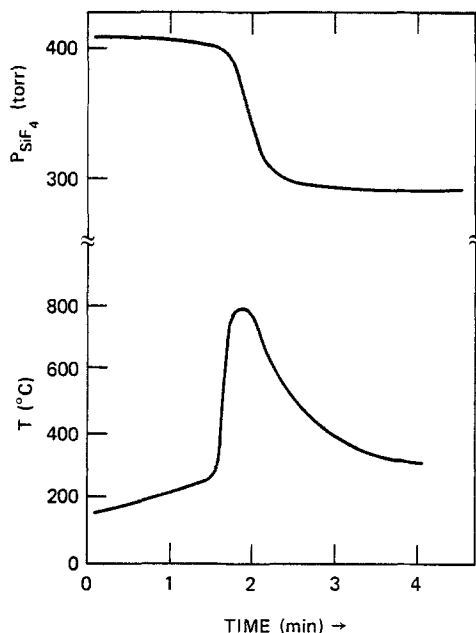


Fig. 2. SiF_4 -Na reaction: pressure and temperature profiles

atm. Reaction was initiated as soon as Na chips were dropped to the bottom of the reactor, which was preheated to 400°C . Reaction was sustained by manually adding Na chips at a rate sufficient to maintain a given SiF_4 flow rate, as indicated by an electronic flowmeter. The maximum flow rate used was 380 liters SiF_4 /hr, corresponding to an addition rate of about 1.4 kg Na/hr and a production rate of 0.5 kg Si/hr. During the operation of the Inconel reactor, the temperature of the reactor walls in the region of the reaction products rose to $600^\circ\text{--}650^\circ\text{C}$, as indicated by external thermocouples. The temperature of the nickel liner reached the melting temperature of NaF (998°C), indicated by molten NaF observed on the outside of the nickel liner near seams as the reaction zone progressed upward.

After each SiF_4 -Na run was completed, the reaction products completely occupied the cylindrical space inside the Ni-Grafoil liner. The reaction products were pulverized with plastic equipment, and routine checks were made for the presence of unreacted Na by acid titration. An important parameter regulating the rate and extent of the reaction is the surface-to-volume ratio of the Na feed. For the 18 cm diam Inconel reactor, no unreacted Na was observed in the reaction products even for the highest Na addition rate used (1.4 kg/hr) when the Na chips had a surface to volume ratio of about 20 cm^{-1} .

The relative amounts of Si, NaF, and Na_2SiF_6 were conveniently determined by x-ray diffraction using standard mixtures. The weight fraction of Na_2SiF_6 was determined from the ratio of the peak intensities of Na_2SiF_6 and KCl reference additive. The method is rapid and accurate to about $\pm 5\%$. The presence of Na_2SiF_6 was also cross-checked by thermogravimetry.

The presence of Na_2SiF_6 in the reaction product mixture is an indication of possible side reaction according to



which is the reverse of the decomposition reaction used for SiF_4 generation in step 1 (Fig. 1) of the overall process.

When the reactor walls are kept above 600°C , the formation of by-product Na_2SiF_6 was less than 2 w/o.

Separation (step 3).—The reaction product obtained by the SiF_4 -Na reaction [1] is a porous, brown mass. This intimate mixture of NaF and Si is readily separated by aqueous leaching. The Si product obtained after leaching is a brown crystalline powder with particle sizes ranging from submicrometers up to $150\ \mu\text{m}$. Some of the various morphological forms observed in this powder are shown in Fig. 4. Leaching is performed using 1.0N HCl in a polypropylene container, although other acids such as H_2SO_4 , CH_3COOH , and HF are equally effective. The acid normality can vary in the range 0.1-1.0N without affecting the leaching process, which may be monitored by measuring the F^- and Na^+ concentrations in the leachant using ion selective electrodes. When the F^- concentration is about 10^{-5} mole/liter, leaching is stopped. The acidification of the leach solution is a precautionary measure to prevent increase in local pH due to reaction of H_2O with Na, which could, in turn, result in Si loss by oxidation according to the reaction



It has been determined (6) experimentally that during leaching in 1N acid, Si can be oxidized at an initial rate of 15 weight percent per hour. The rate of oxidation increases with increased F^- ion concentration in solutions

with pH in the range of -0.8 to 10 . The contact time may be minimized by using forced filtration, which yields a 98% complete recovery of Si. Differences in leaching rate due to particle size of the products, temperature of the leaching bath, and amount of stirring were found to be important only during the first minutes of leaching.

Purity of Silicon

Several analytical methods have been used to characterize the very low levels of impurity elements in the silicon leached from the products of SiF_4 -Na reaction [1]. Generally, each of the methods is used at the limit of resolution for several elements. For comparison, a reference sample of high purity Si was analyzed in a similar manner to provide a check of spurious readings caused by sample preparation, background effects, and instrumental limitations. The reference material was commercial polycrystalline semiconductor grade Si with resistivity greater than $1 \times 10^5\ \Omega\ \text{cm}$.

In Table III, the uncertainty in the methods of emission spectroscopy and spark source mass spectrometry has been taken into account by selecting representative average concentrations based on several analyses. A range is indicated for (Fe, Cr, and Cu) where wide variations occur because of its importance, phosphorous was also determined by a wet chemical colorimetric method (5).

Discussion

The process sequence shown in Fig. 1 was selected because of the inherent simplicity of the steps and their independent and combined suitability for scale-up. Some purification occurs during precipitation (step 1, Fig. 1) for Mg, Ca, Al, P, and As due to the high solubility of their fluosilicates and fluosalts. Some concentration takes place for Cr, Fe, and Ni, and this effect

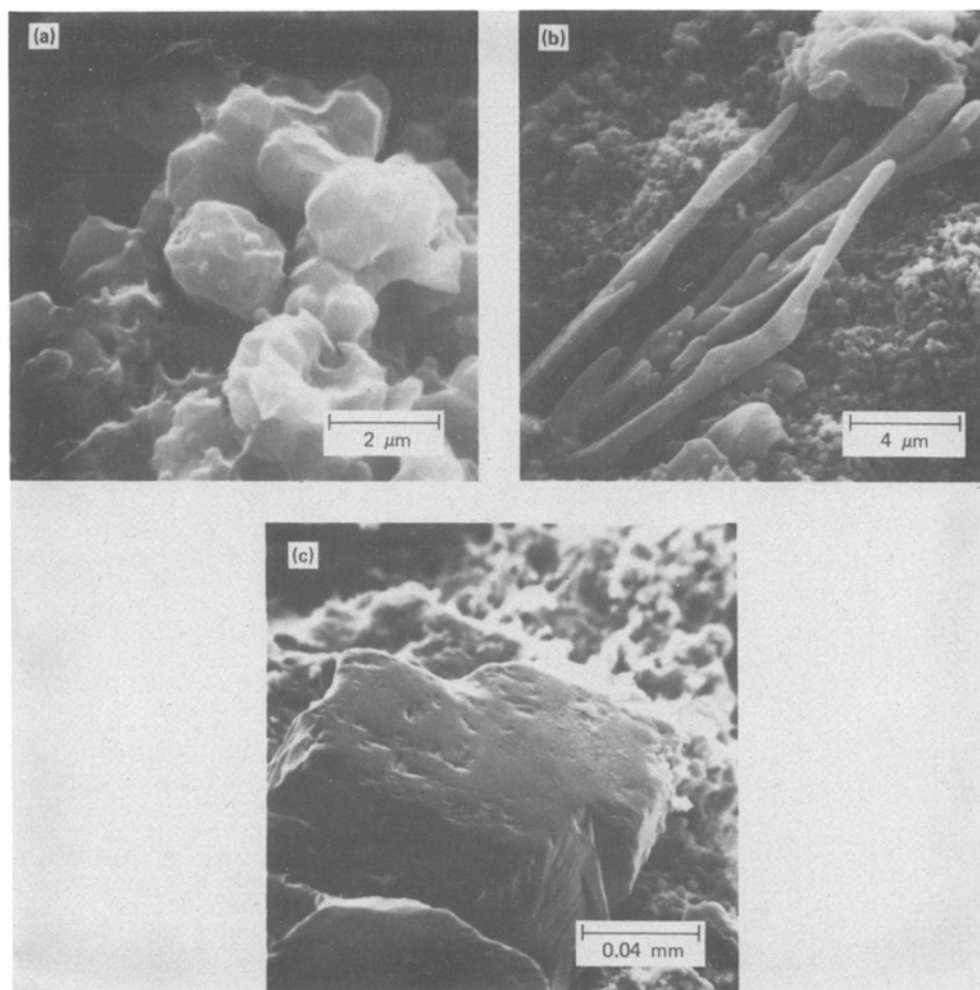


Fig. 4. Morphologies of Si produced in the SiF_4 -Na reaction: (a) fine powder, (b) branches, (c) cubes.

Table III. Representative silicon impurity content, parts per million (wt)

Element	SRI Si ^a	Semiconductor Si
B	0.1	0.1
P	0.2 (0.09) ^b	0.3
As	^c	^c
Al	0.8	0.4
Ga	0.06	0.1
Ti	2.0	0.2
Zr	0.01	<0.3
Mo	0.3	^c
V	0.04	<0.3
Cr	<3.5 ^d	0.8
Mn	0.1	^c
Fe	<7 ^d	<0.3
Co	0.5	0.5
Ni	2.0	4
Cu	<4 ^d	0.2
Zn	0.01	15
F	0.1	<0.1
Na	1.0	9.0
K	0.01	<0.1
Ca	1.0	0.1
Mg	0.1	^c

^a Polycrystalline silicon for single crystal growth.

^b Wet chemical analysis.

^c Not observed.

^d Emission spectroscopy; all others, spark source mass spectrometry.

may be due to coprecipitation of these elements as fluorides since their fluosilicates are very soluble. From Table II, it is clear that most of the purification is accomplished as a result of the thermal decomposition in step 1 (Fig. 1). Most transition metal fluorides are very stable condensed phases at 650°C, the temperature of decomposition in step 1 (Fig. 1) and, therefore, will stay in the solid. In addition, volatile fluorides formed during the decomposition of fluosalts such as Na₂TiF₆ and Na₂ZrF₆ will condense upon cooling of the SiF₄ gas stream from step 1. The condensed material is then removed from the gas mainstream by in-line fume particle filtration. Mass spectrometry did not detect the presence of any metallic or dopant impurity (Table I) in either the SRI produced gas or in the commercial SiF₄ gas. The analysis done on the SiF₄ by passing the gas through high purity water was based on the hypothesis that fluoride impurities should be hydrolyzed and/or trapped in the SiO₂ formed. The results listed in Table II show that the level of metal impurities in the resulting SiO₂ is so low that, for practical purposes, the SiF₄ can be considered free of metallic impurities.

The Na feed, reactor materials, and possible contamination of the product during handling remain as possible sources of impurities in the Si.

The impurities in Na can be divided roughly into three types according to their tendency to react with SiF₄, as classified by the free energy of reaction. The first type of impurity includes aluminum and elements from the groups IA, IIA, and IIIB. The free energy of reaction of SiF₄ with these impurities ranges from -100 to -200 kcal/mole SiF₄ at room temperature and from -50 to -100 kcal/mole SiF₄ at 1500 K. It is expected, therefore, that even when these impurities are present at the ppm level, they will react with the SiF₄ to form the corresponding fluorides. Subsequently, the fluorides will be dissolved preferentially in the NaF phase. The second type of impurity includes transition metals such as Mo, W, Fe, Co, Ni, and Cu, and the elements P, As, and Sb. These elements exhibit positive free energies of reaction in excess of 100 kcal/mole SiF₄ and are not expected to react with SiF₄. However it is an experimental fact that the silicon resulting from the SiF₄-Na reaction contains amounts of Fe, Ni, and Cr in proportion to the concentration of these elements in the Na feed. The mechanism by which these metals are transferred to the silicon has not yet been studied. In any case, the concentration of Fe, Cr, Ni, and also Ti can be decreased by a factor of about 10⁴-10⁶ for single-pass directional solidification or the

Czochralski crystal-pulling procedures used presently for solar cell manufacture. At the resulting levels, these elements would not be detrimental to solar cell performance (1). Boron represents a third type of impurity. The free energy of reaction of this element with SiF₄ is positive but small (5-20 kcal/mole SiF₄ for temperatures up to 1500 K); therefore, some partial reaction can be expected and B will be distributed between the NaF and Si phases. It is noted that the levels of the dopant elements, B, P, and As in SRI silicon are the same as in the semiconductor silicon used as reference. Since it is convenient to have dopant levels as low as possible to permit flexibility in subsequent doping procedures for semiconductor and solar cell applications, the low B and P content (Table III) of Si produced by the SRI process is of advantage. The possibility of contamination from the reactor materials was minimized by the use of Ni and Grafoil liners (Fig. 3) that completely contained the reaction products and avoided contact or impurity transfer with the reactor walls. The Ni liner served merely as a mechanical retainer for the Grafoil sheet and did not contact the solid mixed reaction product. Both Ni and Inconel were selected for use in the reactor (Fig. 3) because of their stability in the presence of fluoride compounds.

Contamination during handling was, after the Na feed, probably the second most important source of impurity pick up. Airborne dust could have contacted the products either during their removal from the reactor or during sampling. Furthermore, although electronic grade acid and deionized water were used for leaching the NaF, the large volume of liquid used could have contributed to the accumulation of impurity in the silicon. Finally, although the purity of the silicon produced by the SiF₄-Na reaction is appropriate for solar cell manufacture, it is expected that by prepurification of the commercial grade Na used and by avoiding contamination during handling, semiconductor grade silicon could be produced.

Conclusion

We have shown experimentally that high purity Si can be prepared as a powder using the inexpensive starting materials H₂SiF₆ and Na. Favorable thermodynamics of the reduction step, easily controlled kinetics, and abundant availability of inexpensive starting materials make this method attractive. Of special interest for semiconductor applications are the low concentrations of B and P impurities in the product Si. The Si produced by the SiF₄-Na reaction, if purified further by directional solidification, should be a low cost material suitable for the manufacture of solar cells.

Acknowledgments

The authors thank Dr. D. Hildenbrand, Dr. K. Lau, and Dr. R. Kleinschmidt for mass spectroscopy work, E. Farley for x-ray work, R. Weaver, S. Leach, S. Westphal, and G. Craig for their cooperation, and Dr. R. Lutwack and Dr. R. Rhein for their comments and suggestions. This work was performed for the Jet Propulsion Laboratory, California Institute of Technology, and was sponsored by the U.S. Department of Energy under Contract DOE/JPL-954471 by agreement with NASA.

Manuscript submitted Feb. 12, 1979; revised manuscript received July 21, 1980.

Any discussion of this paper will appear in a Discussion Section to be published in the December 1981 JOURNAL. All discussions for the December 1981 Discussion Section should be submitted by Aug. 1, 1981.

Publication costs of this article were assisted by SRI International.

REFERENCES

1. R. H. Hopkins, R. G. Seidenstecker, J. R. Davis, P. Rai-Choudhury, P. D. Blais, and J. R. McCormick,

- J. Cryst. Growth*, **42**, 493 (1977).
 2. J. W. Chem, A. G. Milnes, and A. Rohatgi, *Solid-State Electron.*, **22**, 801 (1979).
 3. Proceedings of the 10th LSA Project Integration Meeting, August 16-17, 1978, JPL Document 5101-86, p. 2-3.

4. H. E. Balke *et al.*, Report of Investigation No. RI 7502, U. S. Bureau of Mines (April 1971).
 5. Balazs Analytical Laboratory, Mountain View, California.
 6. K. M. Saucier and V. K. Kapur, *This Journal*, **127**, 1849 (1980).

Surface Conversion for Antisticking to Reduce Patterning Defects in Photolithography

Toshiharu Matsuzawa, Hiroshi Yanazawa, and Norikazu Hashimoto

Hitachi Limited, Central Research Laboratory, Kokubunji, Tokyo 185, Japan

and Hiromitsu Mishimagi

Hitachi Limited, Device Development Center, Kodaira, Tokyo 187, Japan

ABSTRACT

After an exhaustive reevaluation of the contact printing processes, photoresist sticking to the photomask surface is identified as the principal cause of patterning defects and a preventive measure is developed. This process, called surface conversion for antisticking (SURCAS), facilitates a reduction in defect density by about one-fourth compared to conventional contact printing. This technique opens the way for improvement of current LSI fabrication, and moreover should be useful in ultrafine pattern lithography down to 1 μm in the near future.

Photolithographic technology has been successively improved and has dominantly contributed to an increase in LSI packing density by almost a factor of two every year over the last decade. On the other hand, it has also been shown (1, 2) that low device yield is mainly due to patterning defects formed in photolithography. Presently, LSI's with lines and spacings of 3 μm or less are just going into commercial production. When positive photoresists, instead of negative ones, are used in combination with a contact printer, it seems rather easy to delineate 1 μm fine patterns. However, patterning defects due to fragility of the base resin itself have appeared as the most serious problem. Therefore, a new technique to reduce patterning defects is urgently needed to fully utilize the high resolution of positive photoresists for LSI fabrication. In the last several years, great progress has been made by using a 1:1 projection aligner in yield improvement. Still, its resolution limit is recognized to be about 2 μm .

In this work, the contact printing process is reexamined in detail focusing on patterning defects. The investigation has revealed that sticking of photoresist pieces on photomask surfaces is the dominant contributor. This photomask to photoresist adhesion phenomenon is analyzed based on the dry adhesion mechanism reported earlier (3). And finally, a novel technique to effectively prevent sticking, *i.e.*, surface conversion for antisticking (SURCAS), is developed.

Theoretical Treatment

It has become a matter of common knowledge that photoresist to substrate adhesion is improved by surface conversion of substrate wafers with organic compounds such as HMDS.¹

Our experiments revealed an inconsistent phenomenon; when the same conversion treatment is applied to a photomask surface, photoresist to photomask adhesion is drastically weakened. This inconsistency is solved by two different adhesion mechanisms, dry and wet adhesion (3).

Key words: photolithography, contact printing, patterning defects, adhesion, surface conversion.

¹ Hexamethyldisilazane: $(\text{CH}_3)_3\text{SiNHSi}(\text{CH}_3)_3$

Since there is no liquid in the contact printing process, adhesion in photomask-photoresist-substrate system is analyzed according to the dry adhesion mechanism as outlined below. Adhesion between two materials, *i.e.*, photomask to photoresist and photoresist to substrate wafer, is evaluated by dispersion interaction as follows

$$W_{a(\text{MR})} = 2(\gamma_{\text{M}}^{\text{d}}\gamma_{\text{R}}^{\text{d}}) \quad [1]$$

$$W_{a(\text{MR})} = 2(\gamma_{\text{R}}^{\text{d}}\gamma_{\text{S}}^{\text{d}}) \quad [2]$$

where the suffixes M, R, and S denote the photomask, photoresist, and substrate wafer respectively, W_a is the work of adhesion indicating the affinity between two materials denoted by suffixes, and γ^{d} is the dispersion component of surface free energy. Since adhesion increases with W_a , the photoresist will stick to the photomask rather than the substrate when

$$W_{a(\text{MR})} > W_{a(\text{RS})} \quad [3]$$

Substituting formulas [1] and [2] into [3] produces

$$\gamma_{\text{M}}^{\text{d}} > \gamma_{\text{S}}^{\text{d}} \quad [4]$$

Consequently, to prevent the photoresist sticking, $\gamma_{\text{M}}^{\text{d}}$ must be smaller than $\gamma_{\text{S}}^{\text{d}}$.

The values of γ^{d} were evaluated for various materials commonly used in the semiconductor industry, as shown in Fig. 1. The most important point is that a conventional chromium mask washed with organic solvents shows a higher γ^{d} value than any other substrate material. Thus, photoresist sticking can be expected with the above consideration. On the other hand, γ^{d} of the SURCAS mask is the lowest, indicating a low adherence to photoresist.

Experimental

Wafer inspection.—Two series of wafer inspection tests were carried out with each object. The first series was to classify the patterning defects in conventional processes. The second was for yield comparison with and without SURCAS. In the first series, 20 wafers, each including 80 chips of 9 mm^2 die, are processed